Flow Apportionment in a Manifold by using Genetic Algorithm and Least Squares Regression

Thulasiram A.R., Bura Sreenivas, Sreenivas Jayanti

Abstract— Flow apportionment of a 8-parameter flow manifold is dealt in this paper. We deal with a one-by-four manifold. We have to optimally locate the guide plates. The objective of the work is to minimize the standard deviation of the actual flow rates from the set points by controlling 8 parameters four of which are lengths and four of which are angles of deflection. We take the input as the 50 data points generated by the process of CFD. Using the combination of ordinary least squares and genetic algorithms we develop the minimization algorithm for the objective function. We have successfully evaluated the objective and 8 parameters and found that the algorithm employed in this work yields a solution that is lower than the lowest of the 50 data points. Therefore we concluded that our method works successfully without having the need to resort further to CFD computations.

Keywords—Flow manifold, genetic algorithms, least squares, optimization.

I. INTRODUCTION

Flow manifolds are encountered in a variety of chemical process operations like heat exchangers; fuel cells etc. and their uses are versatile. Optimization algorithms are divided into gradient based algorithms and non-gradient based algorithms and genetic algorithms also come under non gradient based algorithms. The use of genetic algorithms needs a fairly large population solution to start the optimization algorithm. Thus the approach we need to follow is to use the meta models. Elsayed[1], Elsayed & Lacor[2] and Elsayed & Lacor[3] constructed prior CFD simulations using the method of ordinary least squares.

Thulasiram A.R, Research Scholar in the department of Chemical Engineering Indian Institute of Technology Madras, Chennai, India -600036 (Corresponding author, email: ch14d414@smail.iitm.ac.in)

Dr. Bura Sreenivas, associated with the Department of Mechanical Engineering, Indian Institute of Technology Madras, Chennai-600036 for his doctoral degree and is currently working as a Professor and Head of the department of Mechanical Engineering , School of Engineering in Nalla Narasimha Reddy Education society's Group of Institutions, Hyderabad, India-500088 (email: sreenivas.b@nnrg.edu.in)

Dr. Sreenivas Jayanti, Professor in the Department of Chemical Engineering, Indian Institute of Technology Madras, Chennai, India-600036 (email:sjayanti@iitm.ac.in).

Li, Fevens & Krzyz[4] present an automated algorithm for clinical image segmentation. In order to facilitate principal component analysis(PCA) and support vector machine application, they classified the image processing process into two steps. These two steps are learning and segmentation. The images are segmented and then feature extraction is applied for image extraction. Then principal component analysis is applied to these extracted images. The results of PCA are used to train a support vector machine classifier. By training a support vector machine, it would be possible to do any medical image segmentation. The domain of application for clinical image segmentation applies to dental x-rays, chest images, scans in 2-d and 3-d etc..

Among many applications that are possible for PCA like process monitoring, fault diagnosis and model identification, Narasimhan[5] use PCA for model identification. They propose a method by which it becomes possible to obtain a nearly exact estimate of the model and error covariance matrix. They also provide an approach for model order determination and data scaling. The data scaling has been noted and used in this work. In addition to usual PCA, they have also evaluated results using iterative principal component analysis (IPCA). The converging singular values that were obtained from iterative principal component were noteworthy, as the last 3 singular values were close to unity, as per theoretical prediction. However when we don't perform scaling, the singular values were not near unity. This demonstrates the importance of scaling while performing PCA. Shariati-rad and Hasani[6] employed PCA for determining the number of species that form during the equilibrium in the complex metal formation of ions with 1-10-phenantroline. Along with using PCA, they used second order global hard modeling. To compare the results of PCA and second order global hard modeling, they used an alternative technique. This alternative method employs multivariate curve resolution-alternating least squares (MCR-ALS). The results from the both approaches were compared and it was found that PCA and second order global hard modeling is better than MCR-ALS. They have pointed out that among all the methods for rank determination, the use of eigen values based on principal component analysis is the best technique.

Coussement, Gicquel and Parente[7] employ PCA to investigate low dimensional manifold in the combustion process. The usual difficulty arises because it is generally

difficult to couple the manifold with the flow-solver. In order to achieve the coupling, the authors propose a new algorithm called manifold generated by a local PCA (MGLPCA). This algorithm successfully couples manifold generated by PCA with a DNS based flow solver. For manifold identification, they employ a premixed one-dimensional freely propagating hydrogen-air laminar flame. This was performed at a specified equivalence ratio and free gas temperature. They have also used a clustering method where they determine the number of principal components along with the number of clusters in MGLPCA.

Lindau et al.[8] build upon PCA to obtain statistical shape modeling for the virtual assemblies. Virtual assembly technique is useful to consider the mating requirement of various geometric shapes that arise when we join two parts. They have presented a method to achieve this mating. This paper demonstrates how PCA can be extended to larger applications to develop more tailor-made and robust applications that are suitable for the given domain. The application they considered were car-bodies. The virtual assembly tool is employed for geometric simulation of various factors like tolerance in geometry, geometric stability issues etc.. This comes under the category of non-rigid assembly simulations, where is assumed that joined parts are not perfect and have manufacturing deviations.

This paper is a continuation of a more realistic flow optimization of the work carried out by Srinivasan & Jayanti[9] . They used Box complex method, which is a gradient based method as an optimization algorithm while in this work we use evolutionary algorithms for optimization. From the literature it is evident that CFD coupled with genetic algorithms is a versatile strategy but still has not been employed for manifold flow optimization. Till now only Box complex method has been employed for optimization of flow apportionment in a manifold. But that was the trend in the past when the fast computing devices were not available and hence it was not feasible to use computationally demanding methods like genetic algorithms. But in the recent years with the advent of fast computers, it became easy to use methods like genetic algorithms which require heavy calculations. Hence in this work we use genetic algorithm as the evolutionary algorithm and CFD as the evaluation mechanism. Another difference with the work of Srinivasan & Jayanti[9] is that they deal with 3 cases out of which 2 cases are 4-paramter problems that have fixed vane lengths and the third case is 8 parameter problem in which 4 lengths and 4 angles are design variables. However in that work the evaluation of flow apportionment for first two cases is easier as it is not complex. But the 8 parameter problem which is the third case is fairly complex and results have further scope for improvement. Thus in this work we deal with the complex 8-parameter problem extensively which is the third case in the work of Srinivasan & Jayanti[9]. Besides Srinivasan & Jayanti[9], Avvari & Jayanti[10] had also carried a similar work. But the difference is that Avvari & Jayanti[10] employed normal gradient approach which is semi-analytical method, while Srinivasan & Jayanti[9] employed a fully computational method by using Box complex method.

II. PROBLEM FORMULATION

The objective of the present work is to explore the feasibility of utilizing genetic algorithms to the problem of determination of optimal flow distribution in a manifold by positioning the angles of the vanes and constructing the lengths of the vanes. To achieve this, the problem is formulated as a constrained optimization problem whose objective is to minimize the deviation of the actual flow rate from the set point in all the four outlets.

A. Description of geometry of the manifold

The geometric description of the 2-dimensional flow manifold is described in Fig.1. The fluid flow manifold consists of one inlet and four outlets where the breadth of the inlet duct is 0.1 m and that of the four outlet ducts is 0.05 m. The breadth header section is 0.1 m. The outlet ports are placed at a distance of 0.05 m with each other. Extended protruding sections of length 0.5 m at the inlet and 2m at the outlets have been facilitated to achieve fully developed flow. Air at a velocity of 15 m/s is specified at the inlet and 1 atmospheric pressure is specified at the outlets.

Physically it is not possible to exceed the length of the plates by 0.05 m and the angle of the guide vanes cannot be less than 90^0 as there is wall behind it (angles are measured in anti-clockwise direction). However as we see in the following sections more severe constraints are imposed on these parameters.
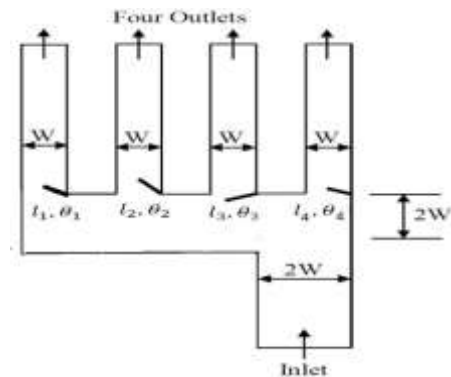

Fig. 1 Schematic of 8-parameter manifold

B. Formulation of the optimization problem

The aim of the current work is to accomplish a predetermined flow apportionment in the outlets. Hence the objective function is given as the additive square root of the deviations of the actual flow rates from the set points in the single channels. The two kinds of parameters which are length and angle of deflection of the guide vanes influence the flow in the manifold and hence the flow apportionment. Hence the objective is obtained as the function of plate parameters. We try to optimize the deviation in the flow apportionment by changing the parameters which are length and angle of the guide vanes. Then, mathematically stating the optimization formulation becomes as:

Minimize f(x) where f(x) = $\sqrt{\Sigma_{j=1}^{q}(Q_j - \breve{Q}_j)^2}$

and x= $\{\theta_i, l_i\}$ (1)

where, q is the total number of outlets, Q_j is the actual flow rate and $\breve{Q}_j$ is the set point of flow rate through the jth stream. x is the parametric set which consists of the angles of deflection θ_i and the lengths of the plates, l_i, for i number of guide plates.

Even though physical realizability limits are different we impose more severe constraints on the parameter values in equation (1) which are as:

$100^0 \leq \theta_1, \theta_2, \theta_3 \leq 350^0$
$100^0 \leq \theta_4 \leq 260^0$
$0.005 \leq l_1, l_2, l_3, l_4 \leq 0.045$

We always obtain non zero flow rates in any channel since the maximum length of the vanes is smaller than the duct breadth.

C. Multi-dimensional ordinary least squares regression using principal component analysis

Regression is the process of fitting a smooth function to a given set of independent data points. That data can be one-dimensional or multi-dimensional. In case the independent variable data is multidimensional then the regression of independent variables to the dependent variable is called multi-dimensional regression. In addition the data can be linear or nonlinear. If the data is nonlinear, then we call the method of regression employed as nonlinear regression.

PCA is a technique used to reduce the number of variables of data into fewer scores and instead of dealing with large number of variables we now deal with fewer number of scores. These scores are stored and subsequently used for further analysis. We can do data recovery or regression using these scores. In case of data recovery, however, based on the number of principal components employed, there is proportional loss in the data. In case of data storage, this is an advantage because sometimes as in case of image processing there is need to store very large amounts of data and due to hardware restrictions we cannot store all the variables and so we need to store only scores.

The case of use of PCA in the case of flow manifold is to reduce redundancy and model the problem effectively. The reason why the modeling is effective is that there are few dominant variables among all the variables which affect the value of the objective function. When we are able to model the objective function as a function of these dominant variables, when can be able to do regression effectively because once accurate model is built, then we can do accurate regression. Since the modeling is based on use of principal components, this type of regression is termed Principal component regression (PCR).In our problem we have 8 independent variables and 1 dependent variable which is the objective function. However some of the 8 parameters are redundant as there are few dominant variables which affect the objective function strongly. The reason why PCA is particularly suitable to this 8 parameter problem is that this 8 parameter case has so many redundancies which reduce the

effectiveness of the modeling phenomenon. PCA addressed such issues by reducing the redundancy. Hence PCR is ideally suited for this 8 parameter problem.

Godoy, Vega, and Marchetti[11] present a detailed comparison between PCA and partial-least squares regression (PLSR) and brings out a relationship between them. They also brought out their utility to various applications like output prediction, modeling and monitoring of multi-variate data. They initially present the geometric properties of the decomposition of input(X-PCA) and output data(Y-PCA) in relation to the PCA. They have achieved the decomposition using partial least squares regression. They have then presented the analogies of data subject to PLSR and YXPCA (input-output PCA). They have concluded that PLSR and YXPCA have similar ability for fault detection. But PLSR was found out to be more reliable for output-prediction, while YXPCA was more reliable for reducing redundancies. They have pointed out that the main difference between YXPCA and PLSR is that YXPCA does not distinguish between inputs and outlet and combines them in a single matrix, while PLSR differentiates between inputs and outputs. They have presented the derivations for the modeling for both PLSR and YXPCA in a separate sub-section. They have presented another section containing the relationship between PLSR and PCA.

D. Evaluation of objective using least squares and optimization using genetic algorithms
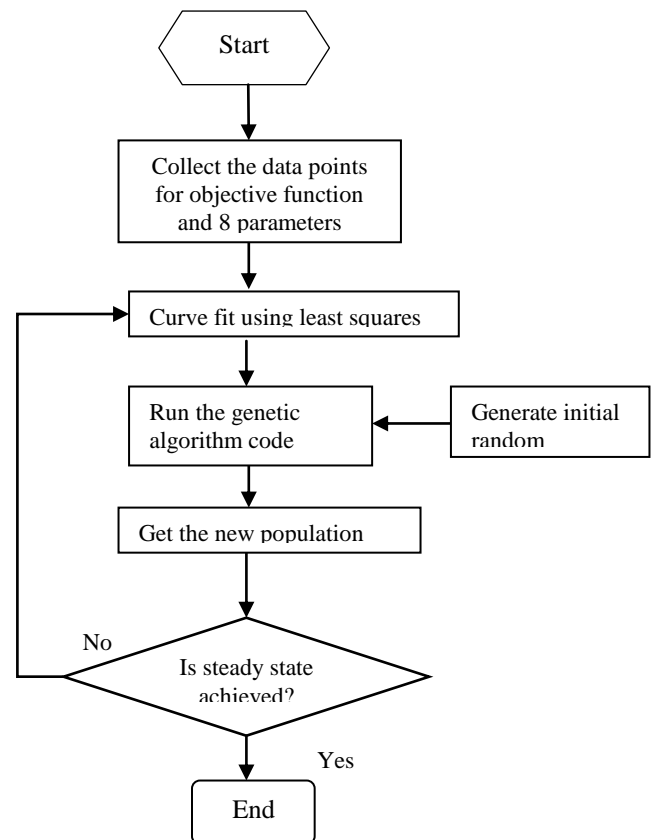

Fig. 2   Flow chart for the optimization code

50 data points are generated using CFD and we do multiple regression to curve fit a model for the data. This model yields the objective function as a function of the 8 design parameters.

Next initial random population is chosen in genetic algorithms. The values of the initial population are evaluated using the objective function that is curve-fitted by ordinary least squares. The optimum is evaluated and next again new population is chosen. This new population is again run through the genetic algorithms code and new objective is evaluated to generate another new population. In this way the code is run through many iterations till the steady state is achieved. The flow sheet is shown in Fig.2.

III. RESULTS AND DISCUSSIONS

50 random data points in 8-dimensions for the 8 parameter problem are generated and the value of the objective function is evaluated in ANSYSFLUENT work bench for the 50 data points. It is noted that each CFD evaluation is computationally expensive and the computational time increases as we try to make the grid finer. The point where we halt for grid refinement is discussed below.

A. Grid refinement and evaluation of objectives

The grid refinement is a very important topic in the CFD based evaluations. Unless the grid convergence is established for a sufficiently fine grid size, we cannot be sure that our results are accurate. The approach we take is that we check the results for a particular grid size, then we reduce the grid size by 25%-75%, check the values if they are same or not. If they are not same we further reduce the grid size. As we make the grid size finer and finer, at one point of sufficient finest grid we can expect the numerical solution to match the analytical solution after which however finer we go the solution remains same. This point is selected for CFD based evaluations. In our case we have initially tried to simulate at 6mm and then do the same simulations for 3mm but the results are not same. Then we tried 3mm and 1.5 mm, still the results varied. We try to

evaluate grid convergence. It was found that grid converges at 1.5 mm. To demonstrate the grid convergence after 1.5 mm we choose two grids 1.5mm and 1 mm values and show that the values obtained by CFD and the plots and graphs are same.

B. Use of genetic algorithms and ordinary least square regression

The angles are in degrees which range between 0 to 360, while the lengths specified are in meters in the range of 0 to 0.045. Before employing genetic algorithms we scale and non-dimensionalize them to maintain uniformity in the code. We choose to non-dimensionalize the angles by 360° and the lengths by 0.05m which is the duct width of the manifold. Fig.3 shows the value of the standard deviation of the flow rates. It can be observed that the standard deviation of the flow reaches a steady value after 190 iterations or generations. It attains a steady state value of 1.2589×10^{-5}. Fig.4 shows the values of the design parameters for this case. As the case of Fig.3, the oscillations are arrested after 168 generations. The final values obtained by the 8 parameters are shown in table 1. These are the values obtained before scaling that are shown in column 3 of table 1. When we scale theta by 360^0 and length by 0.05m, the values obtained are shown in column 4 of table 1.

C. Validation of results using CFD simulations

Once the values of 8 parameters are obtained, we plug these values in CFD software and try to validate the results. We use ICEM software for geometry creation and Fluent for simulations. When we successfully perform CFD simulations, we get the values of the mass fluxes at the four outlets. The value of fluxes obtained for these set of parameters are plugged in MATLAB to compute the value of the objective function.
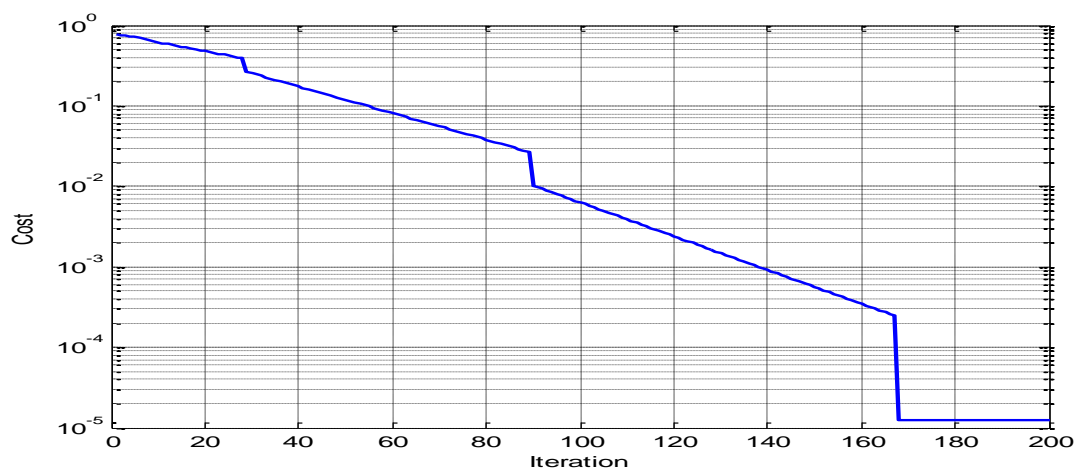

Fig.3   Value of standard deviation before non-dimensionalizing
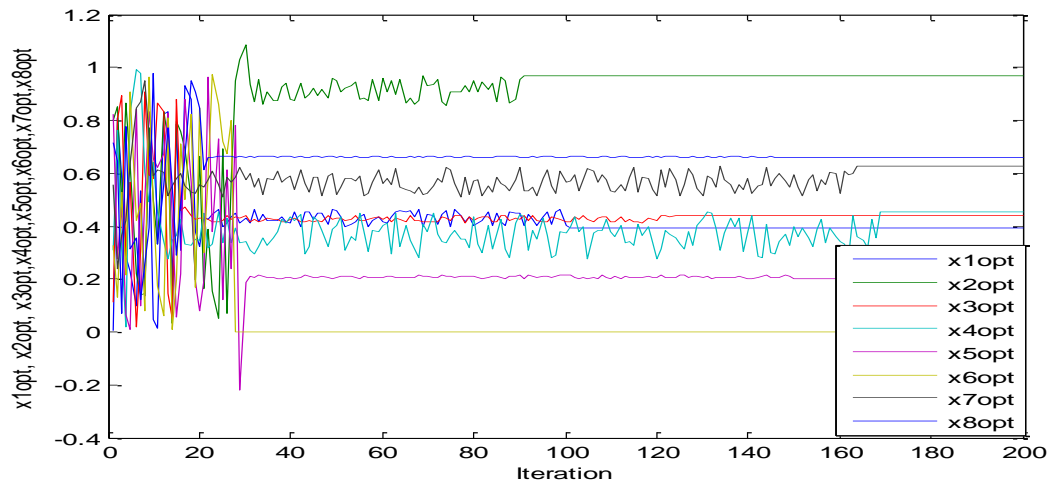
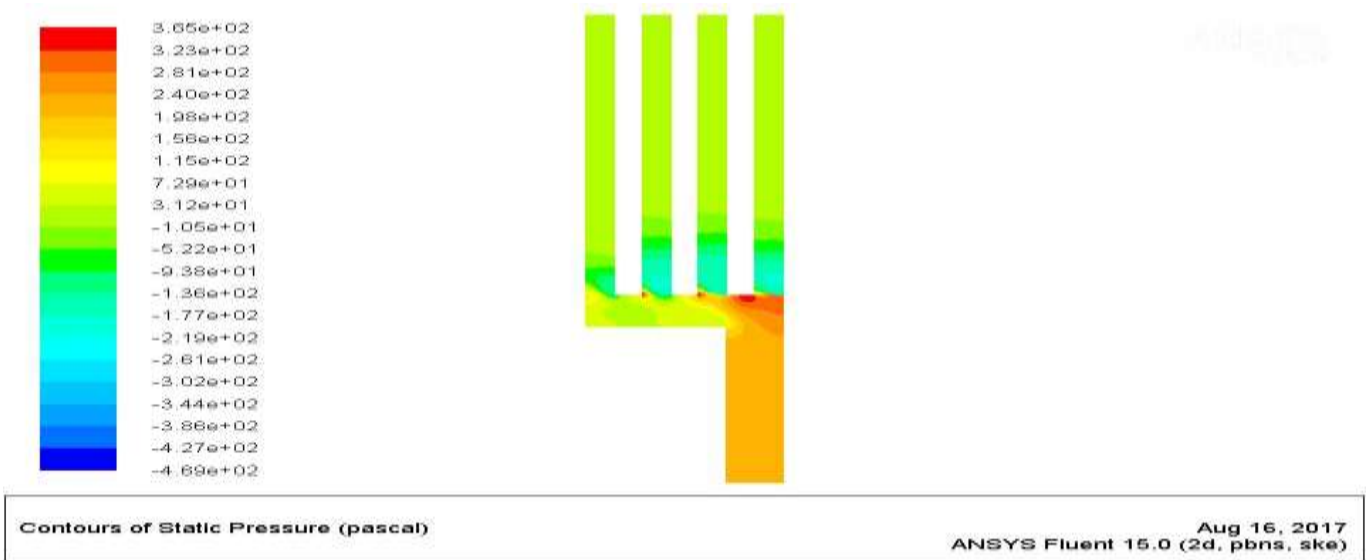Fig. 4   Values of design parameters before non-dimensionalizing
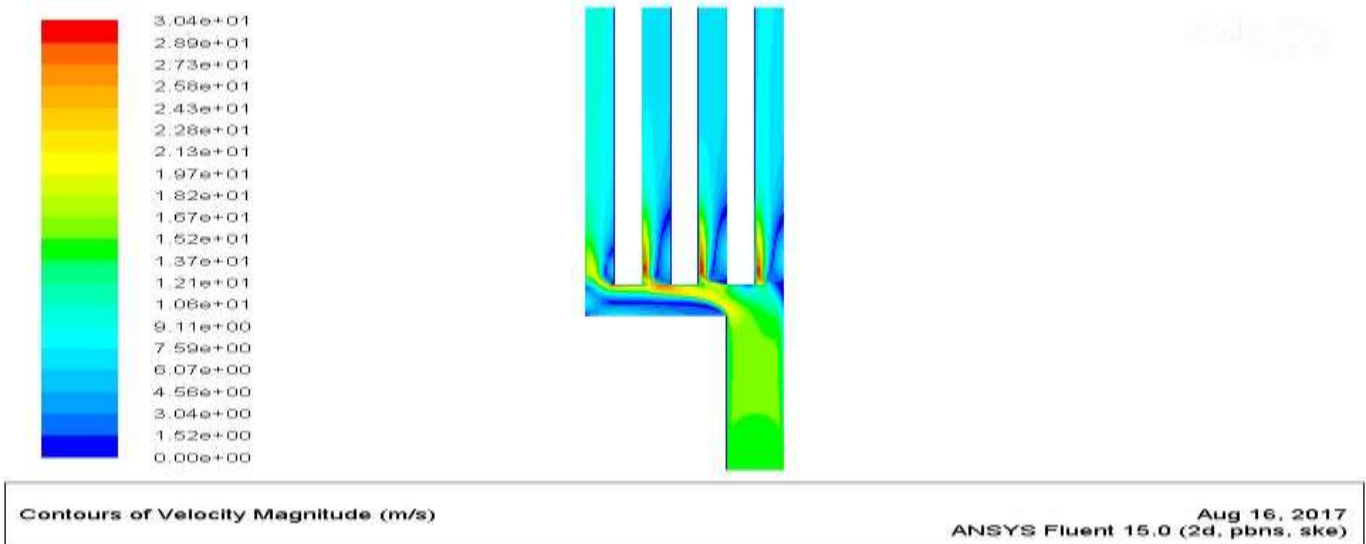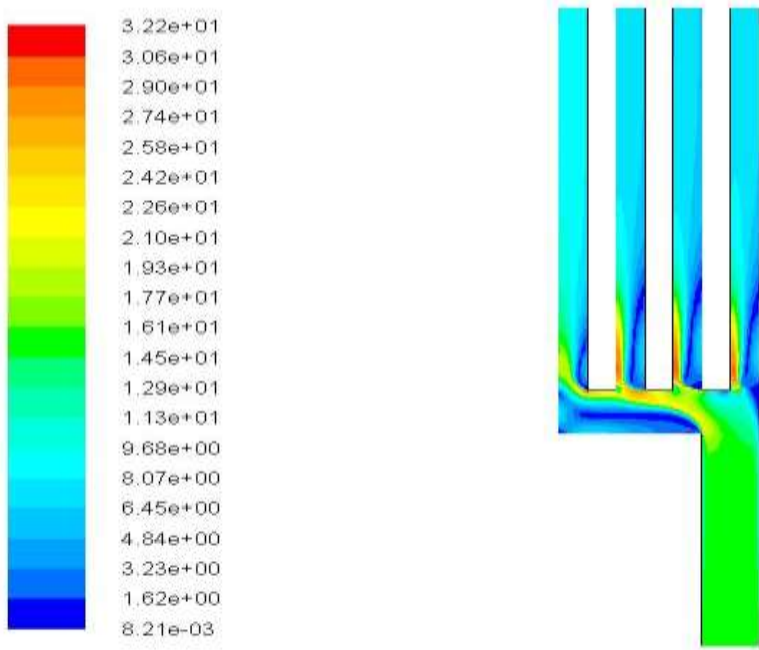

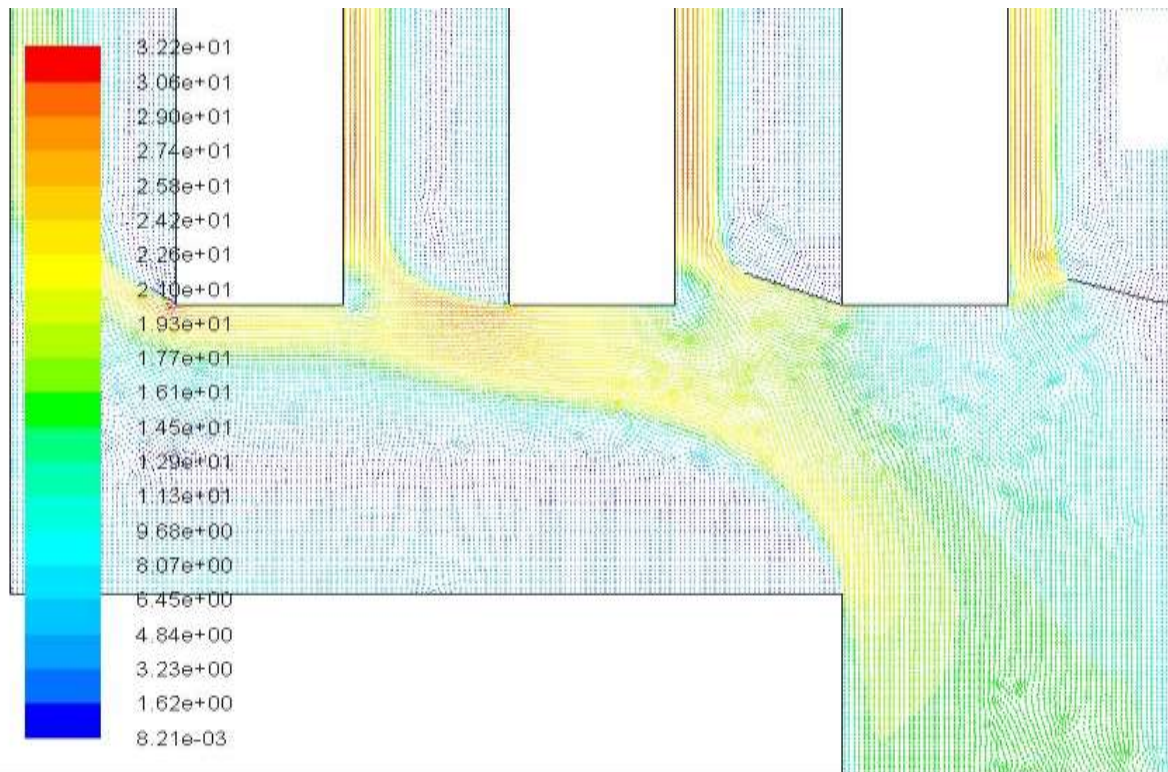Fig. 5 Contours of static pressure for the final result

Fig.6 Contours of velocity for the final result

Fig.7 Velocity vectors for the final result

Fig.8 Velocity vectors in the header

Table 1 Summary of values obtained

S. No.	Variable	Value obtained before scaling	Final values
1	θ_1	0.3944	142.001^0
2	θ_2	0.9700	349.212^0
3	θ_3	0.4420	159.111^0
4	θ_4	0.4556	164.013^0
5	L_1	0.2006	0.01003m
6	L_2	0.0006	0.00003m
7	L_3	0.6258	0.03129m
8	L_4	0.6606	0.03303m
9	Standard Deviation(SD)	-	1.2589×10^{-5}
10	CFD based SD	-	0.0281

The contours of static pressure for the final computed result of Table 1 are shown in Fig.5. It can be observed that there is uniform pressure distribution through all the legs of the manifold. We can observe that regions of low pressure are formed behind the vanes in the outlet leg of the manifolds. This is because low pressure eddies are generated at the back of the manifold. At the entrance of the inlet leg, the pressure is more than the pressure at the exit of the outlet legs. It can also be observed that the pressure at all the four outlet legs is same. The contours of velocity by magnitude are shown in Fig.6. This is also observed to be uniform in all the four legs of the manifold. It can also be observed that the velocity is more at the inlet legs than the outlet legs. In addition it can be observed that the velocity behind the vanes is lowest while the velocity at the openings of the vanes is the highest. The velocity vectors are shown in Fig.7. These are arrows instead of colors. The magnitude of the velocity here is indicated by the length of the arrow. The arrows at the inlet are larger than the arrows at the outlet. It can be observed that the length of

arrows show similar velocity magnitude in all the four legs in the manifold. The zoomed view of the velocity vectors corresponding to Fig. 7 are shown for the header in Fig.8. It can be observed that the size of the arrows is larger in the opening of the outlet created by the vanes, while it is smaller behind the vanes. The Fig. 9-12 give further zoomed view of the velocity vectors in the four legs. Fig. 9 shows the velocity vectors for the first leg. As we can observe that for leg 1, the vane is situated at an angle of 142° to the horizontal in anti-clockwise direction. With respect to the wall the angle is 52°. Then length of the vane is 0.01 m which is 20% of the leg width. We can observe that, near the vane, the flow direction is parallel to the vane. This is because the arrows in front of the vane are parallel to the vane and are pointed in the direction from the inlet to the outlet. However, we can see that this flow direction which is indicated by the direction of arrows is opposite behind the vanes. This indicates reverse flow behind the vanes. We can also observe that within the opening in the entrance of the outlet, as we move farther from the arrows, the flow is directed parallel to the walls. Some of the fluid hits the wall and rebounds back, which is also indicated by the direction and magnitude of the arrows.

Fig. 10 shows the zoomed view of the velocity vectors for leg that is located second from the left side. We can observe that the vane is situated at an angle of 349.212^o to the horizontal in anti-clockwise direction. In clockwise direction, the angle is 10.8^o. The length of the vane is 0.00003 m. It is almost a complete opening in the outlet leg. Most of the fluid flowing from the header is going perpendicular to the vane due to inertia in the direction and hence a very little amount of fluid is flowing into the opening of the outlet leg. It can be also observed that the size of the arrows is larger in the left side than the right side. This happens due to the presence of the wall. It can also be observed that in the right side of the opening within the outlet leg, there is small amount of reverse flow.
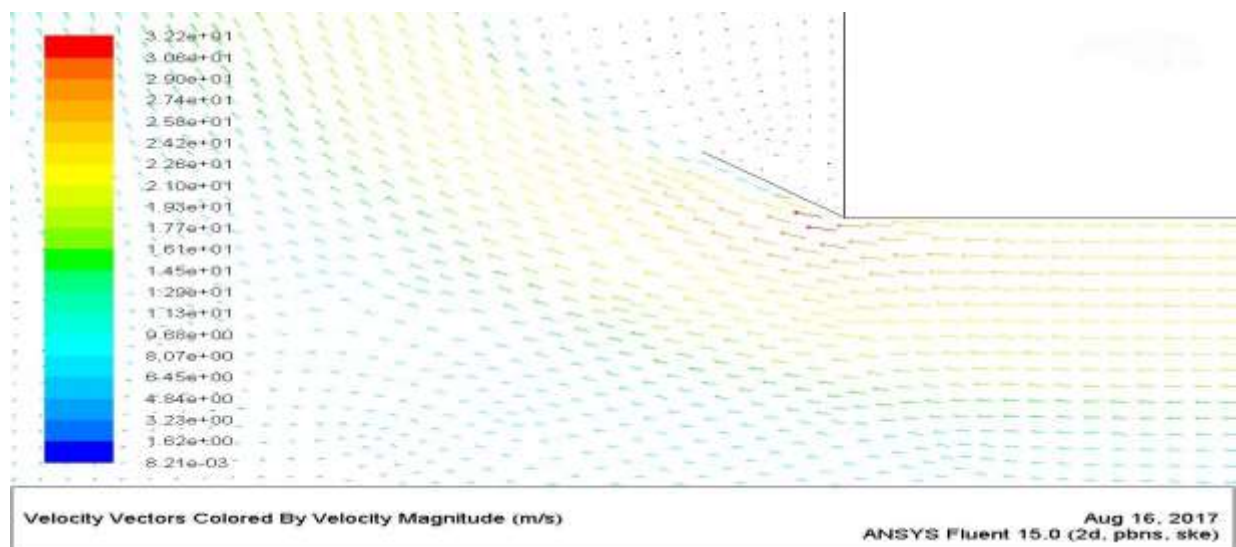

Fig.9 Velocity vectors(zoomed view) in leg 1(left most leg)
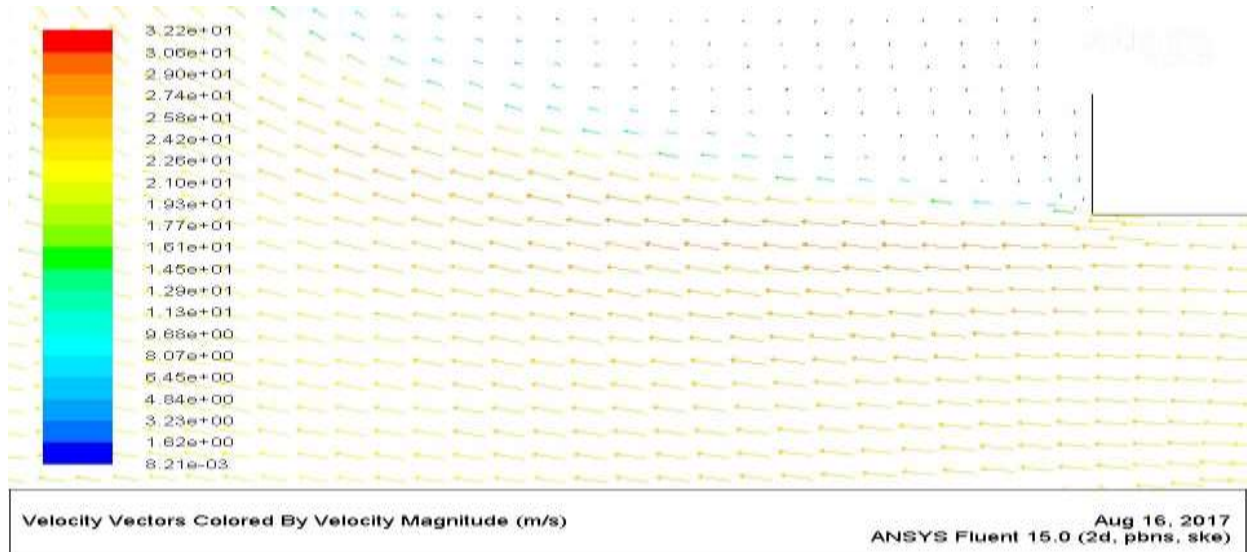
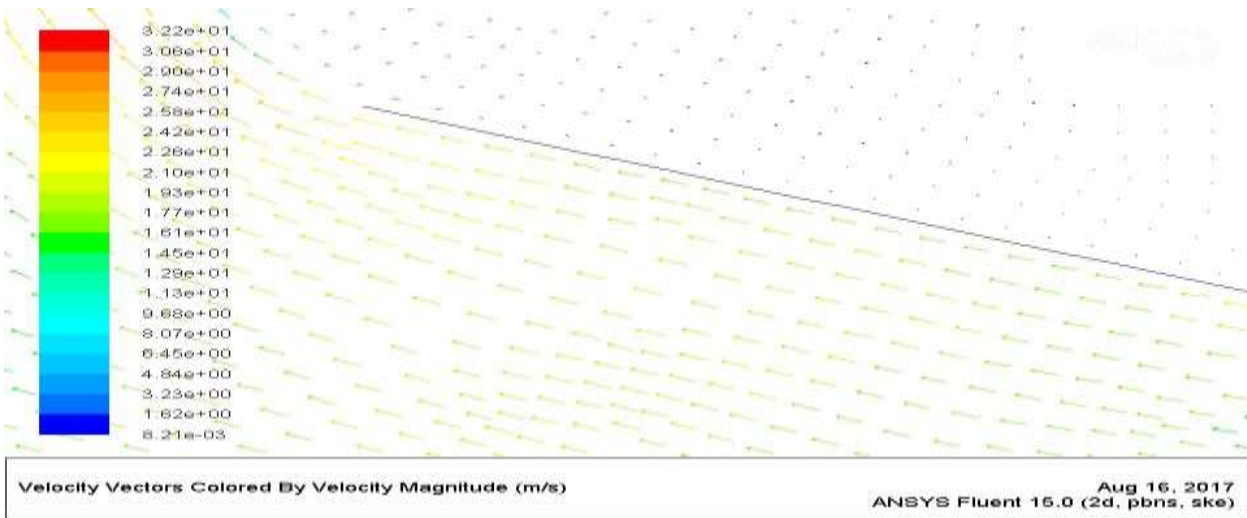Fig.10 Velocity vectors(zoomed view) in leg 2

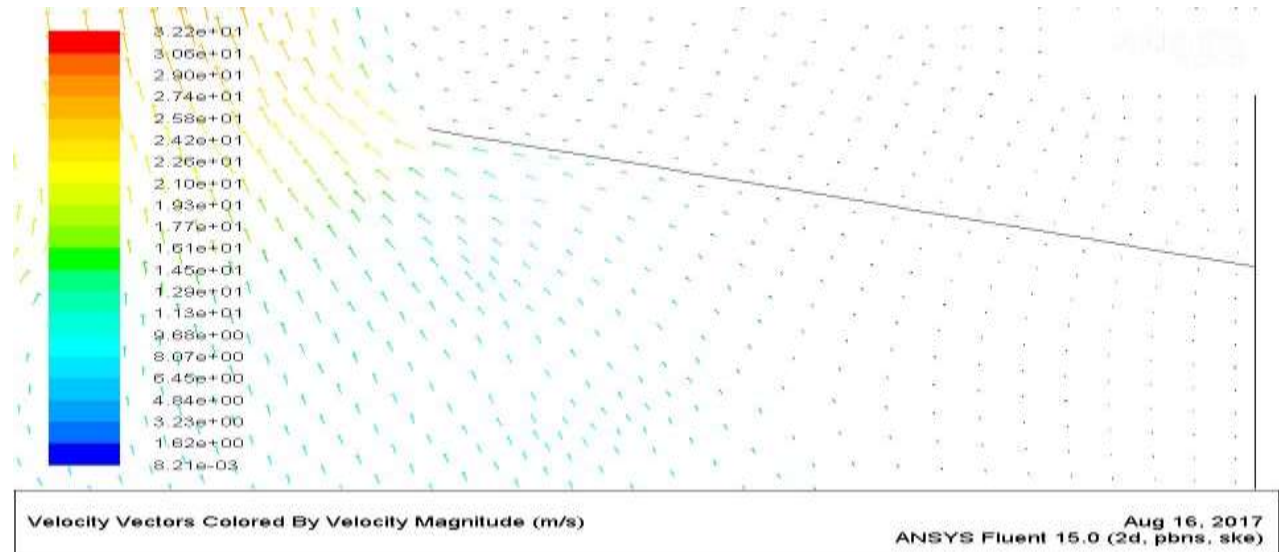Fig.11 Velocity vectors(zoomed view) in leg 3

Fig.12 Velocity vectors(zoomed view) in leg 4(right most leg)

Fig. 11 shows the zoomed view of the velocity vectors in the leg that is situated in third position from the left. The vane is situated at an angle of 159.111^o in the anti-clockwise direction starting from the header wall. With respect to the outlet wall, the angle is 69.111^o. The length of the vane is 0.03129 m which is 63% of the vane opening. We can observe that because the vane is slanted in this case the flow is created in slanting direction and there is good amount of flow inside the opening due to the favorable position of the vanes. It can be also observed that towards the left side of the vane, there is strong magnitude of the flow, while behind the vane there is reverse flow. This illustrates the role of guide vane in the manifold application which is to appropriately control the flow orientation and magnitude. Fig. 12 shows the zoomed view of the velocity vectors in the leg that is situated in fourth position from the left or first position from the right. The vane is situated at an angle of 161.013^o in the anti-clockwise direction starting from the header wall. With respect to the outlet wall, the angle is 71.013^o.The length of the vane is 0.03313 m which is 66% of the vane opening. We can observe that because the vane is slanted in this case the flow is created in slanting direction and there is good amount of flow inside the opening due to the favorable position of the vanes. Since the outlet leg is situated directly in line with the flow inlet leg, we can observe that the flow is coming moving into the outleg leg. The role of guide vane becomes more predominant for this first vane than the other 3 vanes of the other legs. This is because more flow deflection is needed in this leg. It can be observed that in the vicinity of the vane, the flow magnitude is less, as it is rightly indicated by the length of the arrows. There is even small amount of reverse flow, especially behind the vanes and in front of the vanes. But still the flow in the opening to the left of the vane is very large due to inertia of direction from the inlet.

IV. Conclusions

In this paper we use genetic algorithm and modeling through ordinary least squares instead of direct CFD simulations and box complex method to solve for flow minimization in a manifold problem. It has been found that a significant improvement in the standard deviation has been obtained with very less CFD computations. If we observe the standard deviations of the initially chosen 50 random data points, the lowest value is 0.0526. But using our method, we have improvised the solution by achieving a standard deviation of 0.028. Therefore the optimization using genetic algorithms combined with least squares regression has yielded an improvised solution. Further it is noted that we have achieved this result without resorting to computationally expensive CFD simulations. The velocity contours obtained for the final solution through CFD simulations have been demonstrated for illustration.

References

[1]   K. Elsayed, "Optimization of the cyclone separator geometry for minimum pressure drop using Co-Kriging," *Powder Technology*, vol. 269, no. 22, pp. 409–424, 2015.

[2]   K. Elsayed and C. Lacor, "Modeling, analysis and optimization of aircyclones using artificial neural network, response surface methodology and CFD simulation approaches," *Powder Technology*, vol. 212, no. 1, pp. 115–133, 2011.

[3]   K. Elsayed and C. Lacor, "CFD modeling and multi-objective optimization of cyclone geometry using desirability function, Artificial neural networks and genetic algorithms," *Applied Mathematical Modelling*, 2013.

[4]   S. Li, T. Fevens, and A. Krzyz, "Automatic clinical image segmentation using pathological modeling , PCA and SVM," vol. 19, pp. 403–410, 2006.

[5]   S. L. S. Narasimhan, "Model identification and error covariance matrix estimation from noisy data using PCA," vol. 16, pp. 146–155, 2008.

[6]   M. Shariati-rad and M. Hasani, "Analytica Chimica Acta Principle component analysis (PCA) and second-order global hard-modelling for the complete resolution of transition metal ions complex formation with," vol. 648, pp. 60–70, 2009.

[7]   A. Coussement, O. Gicquel, and A. Parente, "MG-local-PCA method for reduced order combustion modeling," *Proceedings of the Combustion Institute*, vol. 34, no. 1, pp. 1117–1123, 2013.

[8]   B. Lindau, L. Lindkvist, A. Andersson, and R. Söderberg, "Statistical shape modeling in virtual assembly using PCA-technique," *Journal of Manufacturing Systems*, vol. 32, no. 3, pp. 456–463, 2013.

[9]   K. Srinivasan and S. Jayanti, "An automated procedure for the optimal positioning of guide plates in a flow manifold using Box complex method," *Applied Thermal Engineering*, vol. 76, pp. 292–300, 2015.

[10]   R. Avvari and S. Jayanti, "Flow apportionment algorithm for optimization of power plant ducting," *Applied Thermal Engineering*, vol. 94, pp. 715–726, 2016.

[11]   J. L. Godoy, J. R. Vega, and J. L. Marchetti, "Chemometrics and Intelligent Laboratory Systems Relationships between PCA and PLS-regression," *Chemometrics and Intelligent Laboratory Systems*, vol. 130, pp. 182–191, 2014.